E4-2025-14

A. D. Efimov [1,2,*], I. V. Koval [1], I. N. Izosimov [3,**]

# HARRIS MODEL AND **IBM** FOR Pu, Cm, Fm, No

Submitted to “Physical Review C”

[1] Admiral Makarov State University of Maritime and Inland Shipping, St. Petersburg, Russia
[2] Ioffe Physical-Technical Institute of RAS, St. Petersburg, Russia
[3] Joint Institute for Nuclear Research, Dubna, Russia
[*] E-mail: efimov98@mail.ru
[**] E-mail: izosimov@jinr.ru

Ефимов А. Д., Коваль И. В., Изосимов И. Н. Е4-2025-14

Модель Харриса и МВБ для Pu, Cm, Fm, No

Для тяжелых четных ядер Pu, Cm, Fm, No описаны энергии ираст-полос в феноменологической модели переменного момента инерции Харриса и в модели взаимодействующих бозонов (МВБ), включая феноменологию МВБ. Также для двух ядер, $^{244}$Pu и $^{248}$Cm, представлены результаты расчетов в расширенной версии МВБ. Сопоставление этих результатов позволило выявить различные зависимости поведения момента инерции от квадрата частоты вращения и получить соответствующие интерпретации их особенностей. В частности, предложена версия, объясняющая ослабление роста момента инерции при спинах состояний больше $24^+$ в ряде ядер.

Работа выполнена в Лаборатории ядерных реакций им. Г. Н. Флерова ОИЯИ.

Препринт Объединенного института ядерных исследований. Дубна, 2025

Efimov A. D., Koval I. V., Izosimov I. N. E4-2025-14

Harris Model and IBM for Pu, Cm, Fm, No

For heavy even nuclei Pu, Cm, Fm and No, the description of the energies of yrast bands in the Harris phenomenological model of the variable moment of inertia and in the interacting boson model (IBM), including IBM phenomenology, is considered. For two nuclei, $^{244}$Pu and $^{248}$Cm, the results of calculations in the extended IBM version are also presented. Comparison of these results made it possible to identify different characteristics of the behavior of the moment of inertia as a function of the square of the rotational frequency and obtain corresponding interpretations of their features. In particular, a version is proposed that explains the weakening of the growth of the moment of inertia for spins of states greater than $24^+$ in a number of nuclei.

The investigation has been performed at the Flerov Laboratory of Nuclear Reactions, JINR.

Preprint of the Joint Institute for Nuclear Research. Dubna, 2025

## INTRODUCTION

The deviation of the energies of the states of the rotational band from the function $I(I+1)$ is traditionally associated with the dependence of the moment of inertia on the rotational angular momentum or on the rotational frequency. The convergence of the expansion of the rotational energy into a series in powers of the rotational frequency is significantly better than that of the expansion in angular momentum [1]. As the angular momentum increases, a significant change in the internal structure of the nucleus can occur. In this case, the use of perturbation theory to determine the variable moment of inertia has a limited scope of application. Since the energies of states, and accordingly the moments of inertia, are determined by many factors, the use of the Harris model [2] in its phenomenological aspect together with other models, as well as microscopic approaches, continues to be of interest.

The Harris model, which is focused on deformed nuclei, operates with such concepts as the moment of inertia of the nucleus and the rotational frequency.

According to [1], the moments of inertia and rotational frequencies for spin $I$ states are defined as $(\hbar\omega)^2 = 4I(I+1)\big(\partial E/\partial I(I+1)\big)^2$ and $2J/\hbar^2 = \big(\partial E/\partial I(I+1)\big)^{-1}$. For the moment of inertia during transitions $I \to I-2$ between adjacent members of the rotational band, the generally accepted expression $2J/\hbar^2 = (4I-2)/E(I \to I-2)$ is adopted, where $E(I \to I-2) = E(I) - E(I-2)$. This expression is called the effective [3] or kinematic moment of inertia [4–6]. At the same time, several representation options are used for the rotational frequency. One of them in [1] has the form $(\hbar\omega)^2 = (I^2 - I + 1)\big(E(I \to I-2)\big)^2/(2I-1)^2$. In another version [3], this expression, presented in Eq. (1), turns out to be closer to the estimate $\hbar\omega = E(I \to I-2)/2$, which is also used in a number of works, see, for example, [5, 7]. In the present work, the expressions accepted are

$$\frac{2J}{\hbar^2} = \frac{4I-2}{E(I \to I-2)}, \quad (\hbar\omega)^2 = \frac{\big(E(I \to I-2)\big)^2}{\Big(\big(I(I+1)\big)^{1/2} - \big((I-2)(I-1)\big)^{1/2}\Big)^2}. \quad (1)$$

The parameterization of the moment of inertia in accordance with [1, 2] is presented as an expansion in powers of $\omega^2$:

$$J = J_0 + J_1\omega^2 + J_2\omega^4 + J_3\omega^6 + \dots \quad (2)$$

with formal parameters $J_0,\ J_1,\ J_2,\ J_3$. The standard deviation characterizing the agreement between the calculated and experimental energies will be determined by the value

$$\sigma = \sqrt{\frac{\sum_I^{I_{\rm fit}}(E_I^{(\rm exp)} - E_I)^2}{I_{\rm fit}/2}}\,, \tag{3}$$

where $I_{\rm fit}$ is the maximum spin of the states of the band up to which the parameters $J_0,\ J_1,\ J_2,\ J_3$ were determined.

In this case, the higher terms in the Harris parameterization themselves do not have physical meaning, but the moments of inertia themselves and their behavior as a function of the square of the rotational frequency do. Confirmation of this can be seen from the parameters $J_2$ and $J_3$ given in Table 1, which determine the moments of inertia, where their values change greatly when moving from nucleus to nucleus. For comparison with the results of Harris's phenomenology, IB$M$1 (Interacting Boson Model) [8], hereinafter simply IB$M$, was used in the traditional way, when its parameters were selected based on the best reproduction of the energies of the collective states. We will call this traditional way of using IB$M$ the IB$M$ phenomenology.

Table 1. **Parameters determining the effective moments of inertia for Pu, Cm, Fm, No isotopes**

| Nucleus | $2J_0/\hbar^2$, MeV$^{-1}$ | $2J_1/\hbar^4$, MeV$^{-3}$ | $2J_2/\hbar^6$, MeV$^{-5}$ | $2J_3/\hbar^8$, MeV$^{-7}$ | $\sigma$, keV | $I_{\rm fit}$ | $I_{\rm max}$ |
|---|---|---|---|---|---|---|---|
| $^{236}$Pu | 133.89789 | 898.00964 | –9071.48730 | 284890.21875 | 0.394 | 24 | 24 |
| $^{238}$Pu | 135.87498 | 680.54706 | –3151.04468 | 41275.67969 | 0.409 | 30 | 30 |
| $^{240}$Pu | 139.78119 | 764.43188 | 1472.78638 | –18989.12695 | 0.232 | 30 | 32 |
| $^{242}$Pu | 134.10948 | 763.40100 | –5481.77002 | 109530.78125 | 0.477 | 24 | 32 |
| $^{244}$Pu | 133.78386 | 191.09700 | 14731.17188 | –80111.30469 | 0.949 | 20 | 34 |
| $^{246}$Pu | 128.27554 | 571.72980 | –4361.00537 | 134614.01562 | 0.005 | 12 | 12 |
| $^{242}$Cm | 142.74765 | 628.33154 | 8013.95605 | –76351.53125 | 0.281 | 24 | 26 |
| $^{246}$Cm | 139.71741 | 655.80249 | –1311.70886 | 122855.18750 | 0.283 | 26 | 26 |
| $^{248}$Cm | 137.93388 | 678.14960 | –6950.13672 | 239460.56250 | 0.134 | 24 | 32 |
| $^{248}$Fm | 130.50784 | 417.03284 | –379.23721 | 33667.18750 | 0.176 | 18 | 18 |
| $^{250}$Fm | 136.22990 | 473.68762 | –1286.68591 | 48557.87891 | 0.133 | 22 | 22 |
| $^{252}$No | 129.13078 | 451.21332 | –4724.84375 | 109247.46094 | 0.199 | 20 | 20 |
| $^{254}$No | 136.40199 | 350.21753 | –1357.69324 | 16564.08203 | 0.274 | 24 | 24 |

The microscopic theory used is a microscopic version of the extended IB$M$ with high multipolarity bosons, described in [9, 10], where the backbending is reproduced. For brevity, we will henceforth refer to it as the microscopic version of IB$M$. Of the nuclei considered below, the structure of the $^{244}$Pu nucleus was calculated in this approach, for which a reverse bending of the moment of inertia at spin $24^+$ is clearly observed and, accordingly, the bands cross. Therefore, in the Harris scheme, calculations of the moments of inertia and excitation energies were made, determining the parameters of the moments of inertia by the states of the yrast band only up to spin $20^+$. The results are shown in Fig. 1, from which it is clear that for states starting with spin $24^+$ the moments of inertia are definitely not reproduced. The same figure shows the results of calculations within the microscopic version of the extended IBM version taking into account high-multipolarity bosons, where the backbending is reproduced. Figure 2 shows the structure of the wave functions of the yrast band states. From this figure it is clear that in the state with spin $22^+$ the three components, namely, the collective and the ones containing bosons with spins $10^+$ and $12^+$, are approximately equal. In the state with spin $24^+$, the main component becomes the one containing the boson with spin $12^+$. This corresponds to the calculation in the Harris scheme, which successfully describes states up to spin $22^+$. If for $^{222}$Th the Harris scheme successfully reproduces collective states in which the collective component is maximal of all others [11], then for the nucleus under consideration three components are significant at the intersection point (at spin $22^+$) and this somewhat shifts the applicability of the Harris scheme to larger spin values.

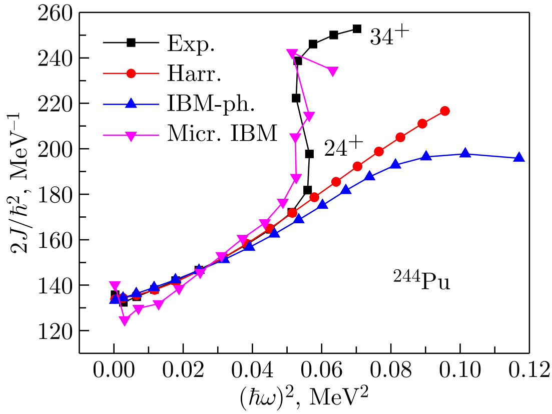


Fig. 1. Moments of inertia for the yrast band based on the microscopic model for $^{244}$Pu, where the effective values are given, corresponding to the experimental energies and those obtained in the Harris scheme in such a way that the corresponding parameters were selected for the states from the lowest to those indicated. Those corresponding to the microscopic calculation are also given

By comparing the results of calculations obtained within the IBM microscopic version, in the IBM phenomenology and in the Harris scheme with experimental data, it is possible to make judgments about the nature of the states under consideration up to the limit of observable spins. It also

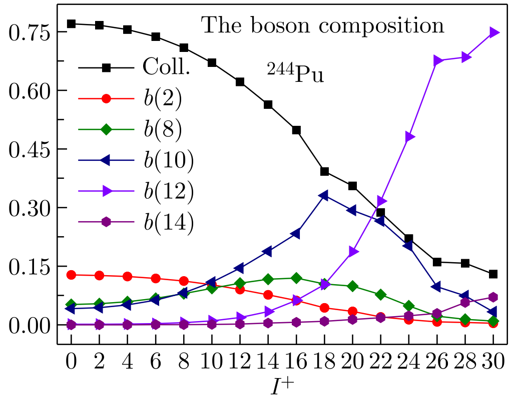


Fig. 2. The composition of the wave functions of the states of the yrast band obtained on the basis of the microscopic model for $^{244}$Pu

provides clear guidelines for subsequent microscopic calculations of the nuclei considered below.

The IBM Hamiltonian used is taken as

$$H_{\mathrm{IBM}} = \varepsilon_d\ \widehat{n}_d + k_1(d^+\cdot d^+ ss + \mathrm{H.c.}) + k_2\left((d^+d^+)^{(2)}\cdot ds + \mathrm{H.c.}\right) + \\ + \frac{1}{2}\sum_L C_L (d^+d^+)^{(L)}\cdot(dd)^{(L)}, \quad (4)$$

where H.c. means Hermitian conjugation, the dot between the operators corresponds to the scalar product, and the quantities $\varepsilon_d$, $k_1$, $k_2$, $C_0$, $C_2$, $C_4$ are the parameters of the model. The total number of bosons or the maximum number of $d$ bosons is denoted by $\Omega$. This Hamiltonian is the traditional IBM Hamiltonian, except for a number of terms, for example, $s^+s^+ss$, which are not considered here. Since it describes the structure of collective states from vibrational to rotational, the parameter $\varepsilon_d$, called the one-boson energy, can be either positive or negative. The latter is invariably realized for deformed nuclei.

## 1. ANALYSIS OF MOMENTS OF INERTIA FOR EVEN Pu ISOTOPES

The moments of inertia for even isotopes of plutonium are shown in Fig. 3. In addition to the experimental and calculated Harris values of the moments of inertia, the parameters of which are given in Table 1, calculations are given in accordance with the IBM phenomenology without taking into account high-spin modes. The parameters of the boson Hamiltonian are taken to be close to those given in [12], and their values are presented in Table 2. For all plutonium isotopes, except for $^{242,244}$Pu, where there is a backbending of the moment of inertia as a function of the square of the rotational frequency, the description of the energies of the yrast bands and, accordingly, the moments of

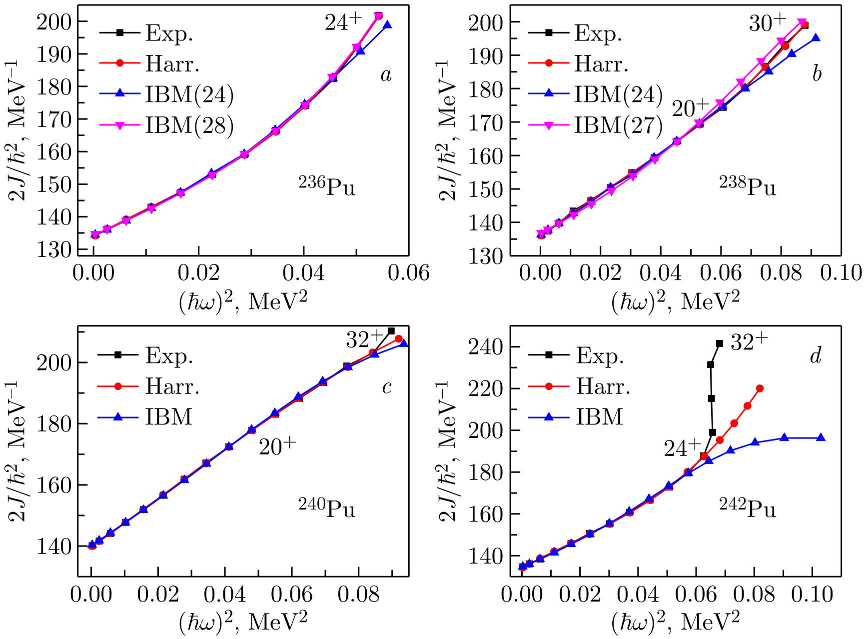


Fig. 3. Effective moments of inertia versus $(\hbar\omega)^2$ for the yrast bands in Pu isotopes from experimental and theoretical energy values

inertia in the Harris scheme is obtained with a high degree of agreement with the experimental data. For the ultimate observed spins, the energies obtained at IBM slightly exceed the experimental ones. This is natural, since as the spin of collective states increases, the influence of high-spin modes on them increases. This leads to an increase in non-collective components in the states as the spin increases. As long as the collective component is larger than the non-collective component, the Harris scheme achieves good reproduction of the experimental data. That is, the influence of non-collective modes on the energies of states is effectively taken into account.

For $^{236}$Pu, as can be seen from Fig. 3, *a*, some upbending of $J(\omega^2)$ is observed at spins $22^+$ and $24^+$. This behavior is reproduced in the Harris model. Within the IBM phenomenology, this behavior is well reproduced, as can be seen from the same figure when increasing $\Omega$ from 24 to 28. The corresponding parameters of the IBM Hamiltonian are given in Table 2. (The parameters of the boson Hamiltonian presented in Table 2 are given with an accuracy of 1 eV as in the work [11], where this is justified. It is due to the requirement that the deviations of the calculated energies should not exceed 0.1 keV within the limits of the used accuracy of the boson parameters.) Thus, the described phenomenon can be associated not with the influence of high-spin modes, but with a feature of purely collective dynamics. Table 3 presents experimental and calculated energies for $^{236}$Pu. The results

Table 2. **Parameters of the IBM Hamiltonian for even nuclei Pu, Cm, Fm, No**

| Nucleus | $\varepsilon_d$ | $k_1$ | $k_2$ | $C_0$ | $C_2$ | $C_4$ | $\Omega$ |
|---|---|---|---|---|---|---|---|
| $^{236}$Pu | −0.849539 | −0.063895 | 0.047109 | 0.795943 | 0.036641 | 0.036367 | 24 |
| $^{236}$Pu | −0.849292 | −0.061687 | 0.042947 | 0.795142 | 0.052083 | 0.025829 | 28 |
| $^{238}$Pu | −0.793156 | −0.050154 | 0.038541 | 0.583019 | 0.097487 | 0.045934 | 24 |
| $^{238}$Pu | −0.803958 | −0.056344 | 0.048141 | 0.617172 | 0.046336 | 0.028484 | 27 |
| $^{240}$Pu | −0.705021 | −0.053353 | 0.043054 | 0.701623 | 0.090824 | 0.039201 | 24 |
| $^{242}$Pu | −0.830231 | −0.061721 | 0.048603 | 0.764612 | 0.032435 | 0.040341 | 24 |
| $^{244}$Pu | −0.804107 | −0.062369 | 0.061048 | 0.596084 | 0.021146 | 0.023194 | 24 |
| $^{246}$Pu | −0.792760 | −0.060414 | 0.052828 | 0.620469 | 0.043172 | 0.029228 | 24 |
| $^{242}$Cm | −0.830573 | −0.058087 | 0.047832 | 0.676933 | 0.058992 | 0.036823 | 24 |
| $^{242}$Cm | −0.821038 | −0.059302 | 0.056414 | 0.572719 | 0.052180 | 0.034578 | 21 |
| $^{246}$Cm | −0.733828 | −0.053350 | 0.041993 | 0.635551 | 0.068013 | 0.036668 | 24 |
| $^{246}$Cm | −0.617604 | −0.047342 | 0.034695 | 0.589696 | 0.054867 | 0.023009 | 30 |
| $^{246}$Cm | −0.686401 | −0.046086 | 0.028129 | 0.584764 | 0.053054 | 0.020616 | 34 |
| $^{248}$Cm | −0.654687 | −0.060535 | 0.058870 | 0.686736 | 0.041507 | 0.024354 | 23 |
| $^{248}$Cm | −0.633889 | −0.058588 | 0.058790 | 0.632129 | 0.032434 | 0.017853 | 25 |
| $^{248}$Cm | −0.607220 | −0.058036 | 0.055955 | 0.644844 | 0.030109 | 0.010808 | 28 |
| $^{248}$Cm | −0.614271 | −0.057803 | 0.052735 | 0.667187 | 0.031646 | 0.008718 | 30 |
| $^{248}$Fm | −0.950121 | −0.058770 | 0.037009 | 0.816178 | 0.022768 | 0.057664 | 26 |
| $^{248}$Fm | −0.872121 | −0.049194 | 0.022972 | 0.752963 | 0.021967 | 0.039133 | 36 |
| $^{250}$Fm | −0.667707 | −0.045596 | 0.039066 | 0.540356 | 0.091952 | 0.040072 | 26 |
| $^{250}$Fm | −0.548454 | −0.039744 | 0.031580 | 0.560606 | 0.094966 | 0.027426 | 36 |
| $^{252}$No | −0.828446 | −0.062310 | 0.057285 | 0.747561 | 0.073516 | 0.040685 | 24 |
| $^{252}$No | −0.724271 | −0.057179 | 0.052693 | 0.710885 | 0.076059 | 0.024973 | 30 |
| $^{252}$No | −0.662900 | −0.056279 | 0.051471 | 0.710096 | 0.075495 | 0.014636 | 34 |
| $^{252}$No | −0.648571 | −0.061355 | 0.059800 | 0.737179 | 0.077578 | 0.000866 | 36 |
| $^{254}$No | −0.855299 | −0.062269 | 0.058609 | 0.817996 | 0.067244 | 0.049793 | 24 |
| $^{254}$No | −0.730608 | −0.056076 | 0.054448 | 0.789201 | 0.068160 | 0.036318 | 30 |
| $^{254}$No | −0.739397 | −0.056125 | 0.054434 | 0.799470 | 0.068028 | 0.029492 | 34 |
| $^{254}$No | −0.726787 | −0.055936 | 0.054881 | 0.785825 | 0.068812 | 0.024660 | 36 |

obtained within the IBM phenomenology are given with $\Omega = 28$. For ease of comparison, the differences between calculated and experimental energies are also given in all subsequent tables. In this case, if these differences are within the experimental error, then the corresponding cells for them are left unfilled.

For $^{238,240,246}$Pu nuclei, the moment of inertia is largely linearly dependent on the square of the frequency, and this is reproduced in IBM.

T a b l e 3. **Comparison of experimental** [13] **and theoretical energy values in keV for $^{236}$Pu nuclei; for IBM** $\Omega = 28$

| $I^{\pi}$ | Exp. | $E_{\rm cal}$ | $E_{\rm cal} - E_{\rm exp}$ | $E_{\rm IBM}$ | $E_{\rm IBM} - E_{\rm exp}$ |
|---|---|---|---|---|---|
| $2^+$ | 44.63(9) | 44.71 | 0.08 | 44.544 | –0.09 |
| $4^+$ | 147.45(9) | 147.529 | 0.079 | 147.34 | –0.11 |
| $6^+$ | 305.80(10) | 305.6 | –0.2 | 305.82 | |
| $8^+$ | 515.70(22) | 515.36 | –0.34 | 516.31 | 0.61 |
| $10^+$ | 773.5(3) | 772.9 | –0.6 | 774.44 | 0.9 |
| $12^+$ | 1074.3(4) | 1073.85 | –0.45 | 1075.5 | 1.2 |
| $14^+$ | 1413.6(4) | 1413.41 | –0.19 | 1414.6 | 1.0 |
| $16^+$ | 1786.0(5) | 1786.59 | 0.59 | 1787.1 | 1.1 |
| $18^+$ | 2188.0(7) | 2188.62 | 0.62 | 2188.6 | 0.6 |
| $20^+$ | 2615.7(9) | 2615.33 | –0.37 | 2614.9 | –0.8 |
| $22^+$ | 3063.7(10) | 3063.24 | –0.46 | 3062.4 | –1.3 |
| $24^+$ | 3529.6(11) | 3529.52 | –0.08 | 3528.1 | –1.5 |

For $^{238}$Pu, two calculations were performed within the IBM phenomenology with $\Omega = 24$ and 27. The moments of inertia in accordance with the experimental energies for the last three transitions do not give a smooth change from $\omega^2$, but a small kink, which is reproduced in the Harris method. The calculation variant in IBM with $\Omega = 24$ gives a practically strictly linear dependence $J(\omega^2)$ and does not reproduce the experimental kink, as can be seen from Fig. 3, *b*. Increasing $\Omega$ to 27 leads to a smooth growth of $J(\omega^2)$, but the kink is not reproduced again. We believe that the variant with $\Omega = 24$ is preferable, and the increase in $J(\omega^2)$ at spins $I \geqslant 26^+$ can be described by the growing influence of high-spin modes with increasing spin of states. Table 4 compares experimental and calculated energies for $^{238}$Pu.

For $^{240}$Pu, calculations were performed in the Harris scheme and within the IBM phenomenology with $\Omega = 24$. In both cases, an excellent result was obtained, as can be seen from Fig. 3, *c* and Table 5, except for the energy with spin $32^+$. Relating this to the results of calculations for $^{244}$Pu, discussed earlier, it can be assumed that in the state with spin $32^+$ the non-collective component, including the two-quasiparticle mode with momentum $12^+$, can be aligned with the collective one and be no less than 30%.

For $^{242}$Pu, in accordance with the new experimental data and the calculations presented in Fig. 3, *d* for $^{242}$Pu without taking into account the high-spin modes, it should be assumed that at spin $24^+$ the collective component will be aligned with the others, and in the state at $I = 26^+$ the bands will definitely cross. This conclusion again follows from the results presented in Figs. 1 and 2. The calculation results for $^{244}$Pu were discussed earlier in connection with Fig. 1.

T a b l e 4. **Comparison of experimental** [13] **and theoretical energy values in keV for $^{238}$Pu nuclei; for IBM** $\Omega = 24$

| $I^\pi$ | Exp. | $E_{\text{cal}}$ | $E_{\text{cal}} - E_{\text{exp}}$ | $E_{\text{IBM}}$ | $E_{\text{IBM}} - E_{\text{exp}}$ |
|---|---|---|---|---|---|
| $2^+$ | 44.065(15) | 44.087 | 0.022 | 43.959 | –0.106 |
| $4^+$ | 145.936(21) | 145.847 | –0.089 | 145.62 | –0.32 |
| $6^+$ | 303.36(6) | 303.06 | –0.3 | 302.98 | –0.38 |
| $8^+$ | 512.55(15) | 512.85 | 0.3 | 513.25 | 0.7 |
| $10^+$ | 771.9(5) | 772.08 | 0.18 | 773.2 | 1.3 |
| $12^+$ | 1077.7(5) | 1077.64 | –0.06 | 1079.5 | 1.8 |
| $14^+$ | 1426.4(6) | 1426.48 | 0.08 | 1428.7 | 2.3 |
| $16^+$ | 1815.5(5) | 1815.6 | 0.1 | 1817.7 | 2.2 |
| $18^+$ | 2241.7(6) | 2242.03 | 0.33 | 2243.7 | 2.0 |
| $20^+$ | 2702.3(8) | 2702.82 | 0.52 | 2703.9 | 1.6 |
| $22^+$ | 3195.4(8) | 3195.11 | –0.29 | 3196.1 | 0.7 |
| $24^+$ | 3717.1(10) | 3716.11 | –0.99 | 3718.5 | 1.4 |
| $26^+$ | 4263.7(11) | 4263.24 | –0.46 | 4269.3 | 5.6 |
| $28^+$ | 4833.3(13) | 4834.09 | 0.79 | 4847.4 | 4.1 |
| $30^+$ | 5426.5(9) | 5426.51 | 0.01 | 5451.9 | 25.4 |

T a b l e 5. **Comparison of experimental** [13] **and theoretical energy values in keV for $^{240}$Pu nuclei; for IBM** $\Omega = 24$

| $I^\pi$ | Exp. | $E_{\text{cal}}$ | $E_{\text{cal}} - E_{\text{exp}}$ | $E_{\text{IBM}}$ | $E_{\text{IBM}} - E_{\text{exp}}$ |
|---|---|---|---|---|---|
| $2^+$ | 42.824(8) | 42.852 | 0.028 | 42.747 | –0.077 |
| $4^+$ | 141.690(15) | 141.712 | 0.022 | 141.47 | –0.22 |
| $6^+$ | 294.319(24) | 294.24 | –0.078 | 293.91 | –0.409 |
| $8^+$ | 497.37(20) | 497.28 | –0.094 | 497.03 | –0.34 |
| $10^+$ | 747.4(3) | 747.31 | –0.093 | 747.36 | |
| $12^+$ | 1041.1(3) | 1040.85 | –0.25 | 1041.3 | 0.2 |
| $14^+$ | 1374.8(4) | 1374.64 | –0.16 | 1375.6 | 0.8 |
| $16^+$ | 1745.7(4) | 1745.79 | 0.09 | 1747.1 | 1.4 |
| $18^+$ | 2151.6(5) | 2151.77 | 0.17 | 2153.1 | 1.5 |
| $20^+$ | 2590.2(5) | 2590.41 | 0.21 | 2591.3 | 1.1 |
| $22^+$ | 3059.8(6) | 3059.9 | 0.1 | 3060.1 | 0.3 |
| $24^+$ | 3559.0(6) | 3558.73 | –0.27 | 3558.0 | –1.0 |
| $26^+$ | 4086.3(6) | 4085.66 | –0.64 | 4084.3 | –2.0 |
| $28^+$ | 4639.4(7) | 4639.74 | 0.34 | 4638.7 | –0.7 |
| $30^+$ | 5220.3(7) | 5220.26 | –0.04 | 5221.3 | 1.0 |
| $32^+$ | 5819.3(8) | 5826.70 | 7.45 | 5832.8 | 13.5 |

For $^{246}$Pu, energies are known only up to spin $I = 12^+$. The dependence $J(\omega^2)$ for this nucleus turns out to be linear, which is reproduced in both calculations.

## 2. ANALYSIS OF EVEN ISOTOPES Cm, Fm AND No

The parameters for the Harris scheme for Cm isotopes are given in Table 1. As can be seen from Fig. 4 and Tables 6–8, the precise reproduction of energies is achieved with an accuracy of 0.6 keV, excluding cases of large experimental error, for the $^{242}$Cm nucleus. In the $^{248}$Cm nucleus up to spin $24^+$, the difference between the experimental and calculated energies does not exceed 0.2 keV. The parameters of the Harris scheme were determined for the corresponding states, as indicated in Table 1.

For $^{242}$Cm, the moment of inertia obtained from experimental data, as can be seen from Fig. 4, *a*, for the second transition gives a noticeable anomaly, which is associated with a large experimental error for the energies of the $4^+$ and $6^+$ levels ($E(4^+) = 137(2)$ keV, $E(6^+) = 288(6)$ keV) (see Table 6). The corresponding anomaly in the moment of inertia leads to the problem of successfully finding the parameters that determine the moments of inertia.

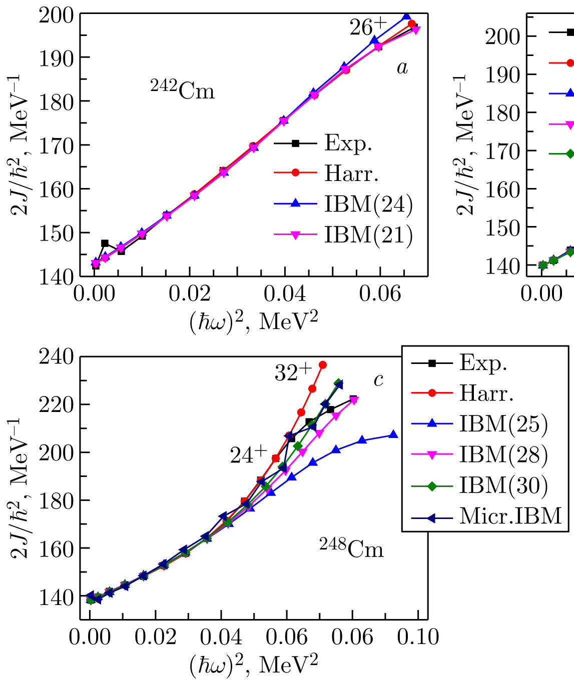


Fig. 4. Effective moments of inertia versus $(\hbar\omega)^2$ for the yrast bands in Cm isotopes from the experimental and theoretical energy values. Micr.IBM data are taken from [10]

Table 6. **Comparison of experimental** [13] **and theoretical energy values in keV for $^{242}$Cm nuclei; for IBM** $\Omega = 21$

| $I^\pi$ | Exp. | $E_{\text{cal}}$ | $E_{\text{cal}} - E_{\text{exp}}$ | $E_{\text{IBM}}$ | $E_{\text{IBM}} - E_{\text{exp}}$ |
|---|---|---|---|---|---|
| $2^+$ | 42.13(5) | 41.978 | –0.152 | 41.935 | –0.2 |
| $4^+$ | 137(2) | 139.04 | 2.04 | 138.92 | 2 |
| $6^+$ | 288(6) | 289.21 | 1.21 | 288.97 | |
| $8^+$ | 489.1(13) | 489.55 | 0.45 | 489.27 | |
| $10^+$ | 735.9(14) | 736.49 | 0.59 | 736.44 | |
| $12^+$ | 1026.2(15) | 1026.29 | 0.09 | 1026.8 | |
| $14^+$ | 1355.2(15) | 1355.38 | 0.18 | 1356.7 | 1.5 |
| $16^+$ | 1720.8(16) | 1720.62 | –0.18 | 1722.7 | 1.9 |
| $18^+$ | 2119.5(17) | 2119.35 | –0.15 | 2121.7 | 2.2 |
| $20^+$ | 2549.3(18) | 2549.43 | 0.13 | 2551.6 | 2.3 |
| $22^+$ | 3008.8(18) | 3009.21 | 0.41 | 3010.8 | 2.0 |
| $24^+$ | 3497.4(19) | 3497.55 | 0.15 | 3499.3 | 1.9 |
| $26^+$ | 4015.7(20) | 4013.78 | –1.92 | 4018.9 | 3.2 |

The situation is corrected if the energies 138.4 and 289 keV are adopted for these states, which are within the experimental confidence intervals and lead to reproduction of the energies of states almost up to spin $26^+$, and $\sigma = 0.28$ keV for states up to $24^+$. For the state with spin $26^+$ in the Harris scheme, the energy turns out to be less than the experimental value. The fact of an additional increase in energies with spins greater than $24^+$ is explained through calculations of these states with different $\Omega$ numbers within the IBM. As can be seen from Fig. 4, *a*, the necessary reduction in the moment of inertia is achieved by reducing the maximum number of quadrupole bosons from 24 to 21. It follows from the same figure that this effect starts with spin $22^+$, manifesting itself as downbending. This is impossible to achieve in the Harris model with the parameterization used. A discussion of this issue will be given below. Table 6 compares the calculated and experimental energies of states in $^{242}$Cm. Calculations of the energies in the Harris scheme within the errors give values that agree with experimental data. At the same time, the relative errors of experimental energies for levels with high spin are smaller than for low-lying states. In this case, using calculations in the Harris scheme can provide a good prediction for experimental refinement of the energies of low-lying states. Calculations in the IBM phenomenology turn out to be of slightly lower quality, but the discrepancies between the calculated values and the experimental ones still do not exceed 2.3 keV, not counting the state with spin $26^+$. The boson parameters found as a result of their fitting, for different values of $\Omega$, are given in Table 2, documenting the presented results.

For the $^{246}$Cm nucleus, the Harris scheme gives a very high quality of reproduction of energies for all states, as can be seen from Table 7. The IBM

T a b l e 7. **Comparison of experimental** [13] **and theoretical energy values in keV for $^{246}$Cm nuclei; for IBM** $\Omega = 34$

| $I^\pi$ | Exp. | $E_{\rm cal}$ | $E_{\rm cal} - E_{\rm exp}$ | $E_{\rm IBM}$ | $E_{\rm IBM} - E_{\rm exp}$ |
|---|---|---|---|---|---|
| $2^+$ | 42.852(5) | 42.883 | 0.03 | 42.877 | 0.025 |
| $4^+$ | 141.989(25) | 141.973 | –0.016 | 142.03 | 0.041 |
| $6^+$ | 294.89(21) | 295.26 | 0.374 | 295.44 | 0.55 |
| $8^+$ | 500.5(5) | 499.97 | –0.531 | 500.20 | |
| $10^+$ | 753.3(6) | 752.75 | –0.551 | 752.83 | –0.5 |
| $12^+$ | 1050.1(7) | 1049.84 | –0.263 | 1049.5 | –0.6 |
| $14^+$ | 1387.1(8) | 1387.13 | 0.0265 | 1386.2 | –0.9 |
| $16^+$ | 1760.2(8) | 1760.36 | 0.157 | 1759.0 | –1.2 |
| $18^+$ | 2165.1(9) | 2165.36 | 0.262 | 2164.1 | –1.0 |
| $20^+$ | 2598.1(9) | 2598.30 | 0.197 | 2597.8 | –0.3 |
| $22^+$ | 3056.0(10) | 3055.77 | –0.232 | 3056.7 | 0.7 |
| $24^+$ | 3535.1(10) | 3534.87 | –0.232 | 3537.6 | 2.5 |
| $26^+$ | 4033.2(11) | 4033.15 | –0.052 | 4037.5 | 4.3 |

for large spins gives energies lower than experimental ones, and the moment of inertia, on the contrary, is correspondingly greater compared to those obtained from experimental data. This is realized at $\Omega = 24$. A successive increase in the maximum number of bosons to $\Omega = 30$ and $\Omega = 34$ brings the experimental and calculated energy values significantly closer even at high spins. Taking into account that the influence of high-spin modes reduces the energies of states with high spins more strongly than with low spins, it can be concluded that in this nucleus the maximum number of bosons should be no more than 34. Taking into account the coupling of collective states with high-spin modes will lower the energies of these states, improving the reproduction of moments of inertia. In the example of $^{246}$Cm, as can be seen from Fig. 4, *b*, the smaller $\Omega$, the more linear the function $J(\omega^2)$ turns out to be.

The situation with the energies of states in $^{248}$Cm is the most complex of all the nuclei considered here, as can be seen from Fig. 4, *c*. The growth of moments of inertia according to experimental data, starting from spin $26^+$, experiences weakening (downbending). Therefore, the Harris parameters were determined by states up to $24^+$ and, accordingly, $\sigma = 0.134$ keV. In order to find out the reasons for this, calculations were carried out at IBM with different numbers of maximum quadrupole bosons. The downbending effect is reproduced at $\Omega = 25$, but the energies themselves, as can be seen from Table 8, starting with spin $18^+$ and going up, exceed the experimental values. As $\Omega$ increases to 30, these differences decrease somewhat, but downbending is no longer reproduced. This is due to the fact that the differences in theoretical energies $E(I) - E(I-2)$ for spins $30^+$ and $32^+$ become smaller

Table 8. **Comparison of experimental [13] and theoretical energy values in keV for $^{248}$Cm nuclei, for IBM variant with $\Omega = 25$, fit until $18^+$**

| $I^\pi$ | Exp. | $E_{\mathrm{cal}}$ | $E_{\mathrm{cal}} - E_{\mathrm{exp}}$ | $E_{\mathrm{IBM}}$ | $E_{\mathrm{IBM}} - E_{\mathrm{exp}}$ |
|---|---|---|---|---|---|
| $2^+$ | 43.40(3) | 43.432 | 0.032 | 43.404 | |
| $4^+$ | 143.80(21) | 143.745 | –0.055 | 143.80 | |
| $6^+$ | 298.9(3) | 298.91 | 0.011 | 299.17 | 0.3 |
| $8^+$ | 506.4(4) | 506.25 | –0.15 | 506.61 | |
| $10^+$ | 762.8(4) | 762.61 | –0.19 | 762.62 | |
| $12^+$ | 1064.1(4) | 1064.17 | 0.068 | 1063.3 | –0.8 |
| $14^+$ | 1406.2(5) | 1406.37 | 0.168 | 1404.8 | –1.4 |
| $16^+$ | 1784.0(5) | 1784.15 | 0.15 | 1783.1 | –0.9 |
| $18^+$ | 2192.7(5) | 2192.49 | –0.21 | 2194.8 | 2.1 |
| $20^+$ | 2627.1(5) | 2626.90 | –0.20 | 2636.8 | 9.7 |
| $22^+$ | 3083.5(6) | 3083.61 | 0.11 | 3106.6 | 23.1 |
| $24^+$ | 3559.6(6) | 3559.58 | –0.021 | 3602.6 | 43 |
| $26^+$ | 4055.4(7) | 4052.34 | –3.058 | 4124.0 | 58.6 |
| $28^+$ | 4572.4(8) | 4559.93 | –12.47 | 4671.6 | 99 |
| $30^+$ | 5114.0(10) | 5080.74 | –33.26 | 5247.6 | 134 |
| $32^+$ | 5680.7(11) | 5613.46 | –67.24 | 5855.8 | 175 |

than the experimental ones, although the theoretical energies $E(I)$ themselves are even larger than the experimental values. It can be assumed that a good description of the energies can be obtained as a result of the simultaneous implementation of two effects. On the one hand, high-spin quasiparticle modes have an effect, and they are larger than in $^{246}$Cm and begin to manifest themselves noticeably with $I = 18^+$. On the other hand, decreasing the size of the collective space with a decrease in $\Omega$ to 25 leads to an increase in $E(I)$ with $I \geqslant 26^+$. Only simultaneous consideration of these two phenomena is capable of reproducing the experimental energies of the yrast band. In the work [10] it was assumed that $\Omega = 28$ and it turns out to be overestimated, as can be seen from Fig. 4, *c*, which led to an excess of the moments of inertia at $I = 30^+$ and $32^+$. Figure 4, *c* for $^{248}$Cm shows the moments of inertia corresponding to the IBM boson parameters with $\Omega = 25,\ 28,\ 30$, given in Table 2. The calculated energies of the levels in IBM, given in Table 8, correspond to the variant with $\Omega = 25$.

Thus, the influence of the total number of bosons on the behavior of $J(\omega^2)$ has been discovered. In some cases, this may serve as a criterion for choosing $\Omega$, which has not been done before. This phenomenon, i.e., downbending at large spins, can be related, among other things, to collective dynamics through a decrease in the size of the configuration space with increasing spin when its values are large. To demonstrate this, Fig. 5 shows the dimensions of the configuration space of collective states in $SU(6)$ IBM

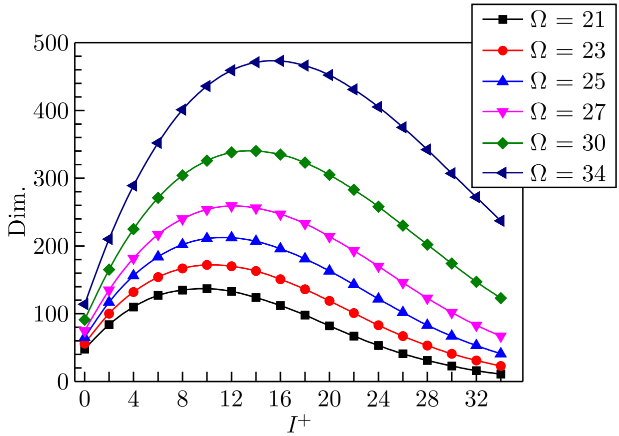


Fig. 5. Dimensions of the boson space of collective states depending on the spin for different values of the maximum number of quadrupole bosons $\Omega$

for different numbers of $\Omega$ depending on the spin. If $\Omega$ is large, then the decrease in the dimensionality of the collective space with increasing spin, starting from $I = 20^+$, is not as noticeable as at smaller values of $\Omega$, or the dimensionality of the space remains significant even at the maximum measured spins. At certain parameters of the Hamiltonian, with increasing $\Omega$, the growth of energies of states with large spins slows down, and the moments of inertia accordingly increase additionally. If the maximum number of bosons decreases, for example, to $\Omega = 23$, then the space of collective states decreases and energies with large spins grow faster than with a large number of bosons, and the moments of inertia fall. The fact that this is not true for all sets of parameters of the boson Hamiltonian is clear from the fact that in the rotational limit of IBM, the energies in the yrast band are proportional to $I(I+1)$, while in the vibrational limit they are proportional to $I$ and do not depend at all on the maximum number of bosons, not counting the cutoff of the band itself after $I = 2\Omega$.

The Harris calculation for $^{248}$Cm at high spins is closest to the IBM calculation with $\Omega > 30$, which does not correspond to the experimental data in terms of the behavior of the energies. The experiment is closer to what the IBM calculation gives with $\Omega = 25$.

A smooth increase in the moment of inertia with increasing spin or rotational frequency can also be realized in purely collective models, in particular, in IBM with a sufficiently large number of bosons $\Omega = 30$ and high spins of at least $24^+$ or $26^+$, as shown in Fig. 4, *c* for $^{248}$Cm. A sharp increase in $J(\omega^2)$ can only be achieved by taking into account high-spin modes. In this case, we will call the corresponding increase in the moment of inertia with increasing rotation frequency “upbending”.

In order to understand how the structure of wave functions changes with spin increase to large values, when the bands do not cross, Fig. 4, *c* also

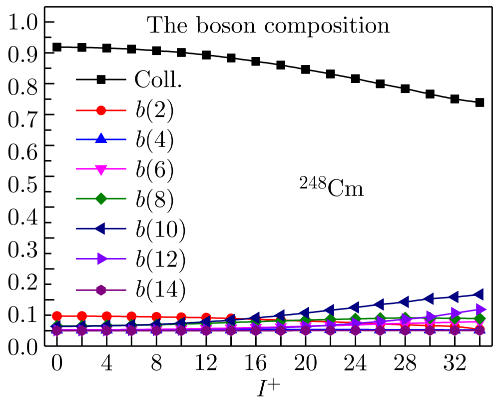


Fig. 6. The composition of the wave functions of the yrast band states, obtained on the basis of the microscopic model for $^{248}$Cm [10]

presents the results of the microscopic version of IBM for $^{248}$Cm, obtained in [10]. They were made with $\Omega = 28$, which led to an overestimated value of the moment of inertia at spin $I = 32^+$. Now it is clear that, by reducing the maximum number of bosons to 25, this can be avoided. Figure 6 shows the calculated structure of the states of the yrast band in $^{248}$Cm [10], from which it is seen that in the absence of band intersection there is a smooth decrease in the wave function component from 92% in the ground state to 74% for the state with $I = 34^+$. In this case, the main non-collective component at extremely high spins becomes the one containing the two-quasiparticle mode with spin $10^+$. In Fig. 6 the contributions to the wave functions from various non-collective states containing modes with spins from $2^+$ to $14^+$ are shown, summed over all corresponding phonons.

Of the Fm isotopes, two are considered, with mass numbers 248 and 250. For $^{248}$Fm, the maximum observed spin is $18^+$ (Table 9), and the scheme of the yrast band levels is reconstructed based on the works [4, 14–16]. It is on the basis of these works that the energy of the $2_1^+$ state was taken to be equal to 44(1) keV, and not 45 keV, as was indicated in the work [6]. The errors indicated in Table 10 correspond only to the errors in the transition energies. The maximally determined spin of the state is $I = 22^+$. Due to such relatively small spins, the Harris scheme gives a precise reproduction of experimental energies with a reserve of data within the possible range of experimental data, see Tables 9 and 10. In Fig. 7, calculations with very different numbers $\Omega$ equal to 26 and 36 are presented for methodological purposes. For $\Omega = 36$, the description of energies and moments of inertia at high spins is somewhat better than for $\Omega = 26$. At the same time, for $^{248}$Fm, the difference between the calculated and experimental energies is noticeably smaller than the experimental uncertainties up to the limiting observed state with spin $18^+$. In $^{250}$Fm, the calculated energies of states with spins $20^+$ and $22^+$ give noticeable excesses over the experimental values. This does not lead

Table 9. **Comparison of experimental** [13] **and theoretical energy values in keV for $^{248}$Fm nuclei, for IBM variant with** $\Omega = 36$

| $I^\pi$ | Exp. | $E_{\rm cal}$ | $E_{\rm cal} - E_{\rm exp}$ | $E_{\rm IBM}$ | $E_{\rm IBM} - E_{\rm exp}$ |
|---|---|---|---|---|---|
| $2^+$ | 46(1) | 45.923 | –0.077 | 45.914 | |
| $4^+$ | 152 | 152.259 | 0.259 | 152.28 | 0.3 |
| $6^+$ | 317.2(3) | 317.28 | 0.081 | 317.34 | |
| $8^+$ | 538.6(4) | 538.53 | –0.069 | 538.58 | |
| $10^+$ | 813.3(5) | 813.04 | –0.26 | 812.95 | –0.4 |
| $12^+$ | 1137.3(6) | 1137.42 | 0.12 | 1137.1 | |
| $14^+$ | 1507.7(7) | 1508.00 | 0.30 | 1507.4 | |
| $16^+$ | 1921(2) | 1920.87 | –0.13 | 1920.5 | |
| $18^+$ | 2372(2) | 2372.03 | 0.026 | 2372.9 | |

Table 10. **Comparison of experimental** [4, 14–16] **and theoretical energy values in keV for $^{250}$Fm nuclei; for IBM** $\Omega = 36$

| $I^\pi$ | Exp. | $E_{\rm cal}$ | $E_{\rm cal} - E_{\rm exp}$ | $E_{\rm IBM}$ | $E_{\rm IBM} - E_{\rm exp}$ |
|---|---|---|---|---|---|
| $2^+$ | 44(1) | 43.994 | –0.006 | 43.983 | |
| $4^+$ | 146(1) | 145.868 | –0.132 | 145.88 | |
| $6^+$ | 303.9(5) | 304.00 | 0.096 | 304.05 | |
| $8^+$ | 515.9(5) | 516.10 | 0.20 | 516.15 | |
| $10^+$ | 779.2(5) | 779.46 | 0.26 | 779.38 | |
| $12^+$ | 1091.0(5) | 1091.03 | 0.034 | 1090.7 | –0.3 |
| $14^+$ | 1447.6(5) | 1447.45 | –0.15 | 1447.1 | –0.5 |
| $16^+$ | 1845.2(5) | 1845.09 | –0.11 | 1845.4 | |
| $18^+$ | 2280.2(5) | 2280.18 | –0.02 | 2282.8 | 2.6 |
| $20^+$ | 2748.8(5) | 2748.96 | 0.16 | 2756.6 | 7.8 |
| $22^+$ | 3247.8(10) | 3247.83 | 0.03 | 3264.2 | 16.4 |

to the crossing of the bands, but it indicates a growing influence of high-spin quasiparticle modes on them. The fact that the crossing of the bands at spin $22^+$ does not yet occur is also indicated by the description of the moments of inertia in this nucleus with the Harris scheme.

Among the nobelium isotopes, the energies of the yrast bands up to high spins are known for two nuclei, these are $^{252,254}$No, respectively, up to spins $20^+$ and $24^+$. As for the Fm isotopes, the Harris scheme gives a precise reproduction of the experimental energies with a reserve of values within the possible range of experimental data (see Tables 11 and 12). At the same time, as can be seen from Fig. 8, for $^{254}$No at small values of $(\hbar\omega)^2$ an

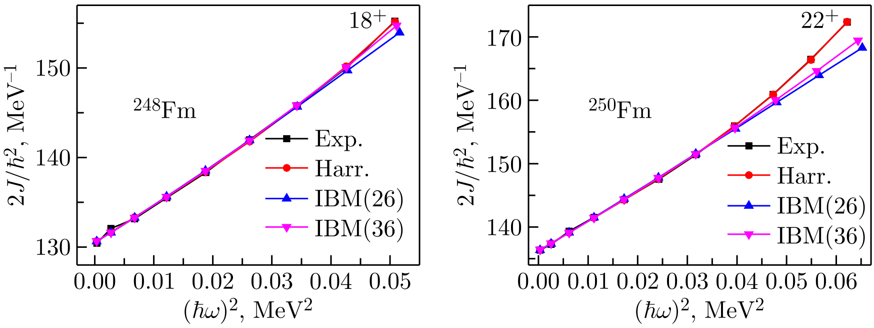


Fig. 7. Effective moments of inertia versus $(\hbar\omega)^2$ for the yrast bands in Fm isotopes from experimental and theoretical energy values

anomaly in $J(\omega^2)$ is observed. It is associated, as in the $^{242}$Cm nucleus, with a large experimental uncertainty (see Table 12). Therefore, both in the Harris calculations and in IBM, the energy values $E(2^+) = 43.94$ keV, $E(4^+) = 145.9$ keV were adopted, which are within the confidence interval of the experimental energies. For $^{252}$No, the calculations in IBM were carried out with $\Omega$ from 24 to 36, which, however, did not improve the description of the moments of inertia for states with spins $18^+$ and $20^+$. At the same time, the experimental and calculated data according to Harris give a noticeable deviation from the linear dependence $J(\omega^2)$, which cannot be achieved in the IBM phenomenology. For $^{254}$No, the experimental dependence $J(\omega^2)$ is closer to a linear one. Therefore, a consistent increase in $\Omega$ in the IBM calculations leads to an improvement in the description of energies up to the state with $I = 24^+$.

Table 11. **Comparison of experimental** [13] **and theoretical energy values in keV for $^{252}$No nuclei; for IBM $\Omega = 36$**

| $I^\pi$ | Exp. | $E_{\mathrm{cal}}$ | $E_{\mathrm{cal}} - E_{\mathrm{exp}}$ | $E_{\mathrm{IBM}}$ | $E_{\mathrm{IBM}} - E_{\mathrm{exp}}$ |
|---|---|---|---|---|---|
| $2^+$ | 46.4(10) | 46.406 | 0.0056 | 46.349 | |
| $4^+$ | 153.6(13) | 153.794 | 0.194 | 153.77 | |
| $6^+$ | 320.6(13) | 320.40 | –0.198 | 320.61 | |
| $8^+$ | 544.4(13) | 543.91 | –0.48 | 544.40 | |
| $10^+$ | 821.6(13) | 821.62 | 0.020 | 822.02 | |
| $12^+$ | 1150.0(13) | 1150.21 | 0.21 | 1149.9 | |
| $14^+$ | 1525.5(14) | 1525.46 | –0.036 | 1524.3 | –1.2 |
| $16^+$ | 1942.2(14) | 1942.30 | 0.10 | 1941.2 | –1.0 |
| $18^+$ | 2395.4(16) | 2395.24 | –0.16 | 2396.6 | 1.2 |
| $20^+$ | 2879.1(18) | 2879.07 | –0.033 | 2886.8 | 7.7 |

Table 12. **Comparison of experimental** [13] **and theoretical energy values in keV for $^{254}$No nuclei, for IBM** $\Omega = 36$**; in the calculations it was taken into account that** $E(2_1^+) = 43.94$, $E(4_1^+) = 145.9$ **keV**

| $I^\pi$ | Exp. | $E_{\rm cal}$ | $E_{\rm cal} - E_{\rm exp}$ | $E_{\rm IBM}$ | $E_{\rm IBM} - E_{\rm exp}$ |
|---|---|---|---|---|---|
| $2^+$ | 44.2(4) | 43.952 | –0.248 | 43.896 | –0.3 |
| $4^+$ | 145.2(7) | 145.93 | 0.73 | 145.84 | 0.6 |
| $6^+$ | 304.6(7) | 304.73 | 0.128 | 304.73 | |
| $8^+$ | 518.7(7) | 518.65 | –0.052 | 518.89 | |
| $10^+$ | 786.0(8) | 785.70 | –0.297 | 786.27 | |
| $12^+$ | 1104.1(8) | 1103.73 | –0.37 | 1104.5 | |
| $14^+$ | 1470.7(8) | 1470.44 | –0.26 | 1471.2 | 0.5 |
| $16^+$ | 1883.4(8) | 1883.40 | 0 | 1883.7 | |
| $18^+$ | 2339.4(9) | 2340.02 | 0.62 | 2339.6 | |
| $20^+$ | 2837.4(14) | 2837.52 | 0.12 | 2836.6 | |
| $22^+$ | 3373.4(17) | 3372.97 | –0.43 | 3372.5 | |
| $24^+$ | 3943.4(20) | 3943.36 | –0.04 | 3945.4 | 2.0 |

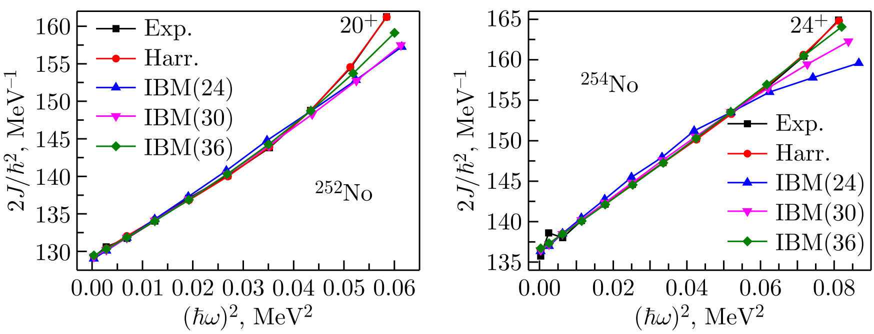


Fig. 8. Effective moments of inertia versus $(\hbar\omega)^2$ for the yrast bands in No isotopes from experimental and theoretical energy values

## CONCLUSIONS

A comparison of the effective moments of inertia for heavy even nuclei Pu, Cm, Fm and No obtained from experimental data with calculations in the model of variable moment of inertia and IBM, both in its phenomenological aspect and in its microscopic version, allowed us to draw the following conclusions.

1) The Harris model effectively reproduces the experimental situation if the collective component in the wave function remains at least 50%. The standard boson model cannot do this and must be extended by explicitly taking into

account high-spin excitation modes. In heavy nuclei, this must be done up to high-spin modes with $J \leqslant 14^+$.

2) If the energies of collective states additionally increase at spins greater than $28^+$, which leads to a weakening of the growth of the moment of inertia or even to a cessation of its growth as the rotational frequency increases — downbending, then this may be due to a reduction of the collective configuration space (the space of $d$ bosons). Such a situation is reproduced in the IBM phenomenology, but cannot be reproduced either in the Harris model or in classical geometric collective models.

3) If upbending is observed according to experimental data and is reproduced in the Harris scheme, then this indicates a noticeable role of high-spin modes, but at the same time the states of the yrast band remain mainly collective. The IBM phenomenology cannot reproduce this, but its microscopic version does.

## REFERENCES


1. *Bohr A., Mottelson B.* Nuclear Structure. New York: Benjamin, 1975. V. 2.
2. *Harris S. M.* // Phys. Rev. B. 1965. V. 138, No. 3. P. 509.
3. *Kusakari H., Kitao K., Sato K., Sugawara M., Katsuragawa H.* // Nucl. Phys. A. 1983. V. 401. P. 445.
4. *Ketelhut S.* Academic Dissertation for the Degree of Doctor of Philosophy, Research Report No. 11/2010, University of Jyvaskyla, 2010.
5. *Hara K., Sun Y.* // Int. J. Mod. Phys. E. 1995. V. 04. P. 637.
6. *Herzberg R. D., Greenless P. T.* // Prog. Part. Nucl. Phys. 2008. V. 61. P. 674.
7. *Jaafer F. A., Al-Khudair F. H.* // Phys. Rev. C. 2022. V. 106. P. 064309.
8. *Arima A., Iachello F.* // Phys. Rev. Lett. 1975. V. 35. P. 1069.
9. *Efimov A. D., Izosimov I. N.* JINR Preprint E4-2024-27. Dubna, 2024.
10. *Efimov A. D., Izosimov I. N.* // Phys. At. Nucl. 2023. V. 86. P. 333.
11. *Efimov A. D., Koval I. V., Izosimov I. N.* JINR Preprint E4-2025-4. Dubna, 2024.
12. *Efimov A. D., Izosimov I. N.* // Phys. At. Nucl. 2021. V. 84. P. 660.
13. National Nuclear Data Center, Brookhaven National Laboratory. http://www.nndc.bnl.gov
14. *Bastin J. E., Herzberg R.-D., Butler P. A. et al.* // Phys. Rev. C. 2006. V. 73. P. 024308.
15. *Herzberg R.-D.* // J. Phys. G: Nucl. Part. Phys. 2004. V. 30. P. R123.
16. *Greenlees P. T., Herzberg R.-D., Ketelhut S.* // Phys. Rev. C. 2008. V. 78. P. 021303(R).


Received on March 31, 2025.

Редактор *Е. И. Кравченко*

Подписано в печать 19.05.2025.
Формат 60 × 90/16. Бумага офсетная. Печать цифровая.
Усл. печ. л. 1,25. Уч.-изд. л. 1,66. Тираж 100 экз. Заказ № 61103.

Издательский отдел Объединенного института ядерных исследований
141980, г. Дубна, Московская обл., ул. Жолио-Кюри, 6.
E-mail: publish@jinr.ru
www.jinr.ru/publish/